Electrochemical Boron-Doped Diamond Film Microcells Micromachined with Femtosecond Laser: Application to the Determination of Water Framework Directive Metals

Amel Sbartai, Philippe Namour, Abdelhamid Errachid, J. Krejci, R. Sejnohova, L. Renaud, M. Larbi Hamlaoui, A.-S. Loir, F. Garrelie, C. Donnet, et al.

Sbartai, A.; Namour, P.; Errachid, A.; Krejči, J.; Šejnohová, R.; Renaud, L.; Larbi Hamlaoui, M.; Loir, A.-S.; Garrelie, F.; Donnet, C.; Soder, H.; Audouard, E.; Granier, J.; Jaffrezic-Renault N., (2012) Electrochemical Boron-Doped Diamond Film Microcells Micromachined with Femtosecond laser: Application to the Determination of Water Framework Directive Metals**, *Analytical Chemistry*, 84, (11), 4805-4811, DOI: 10.1021/ac3003598.**

Electrochemical Boron-Doped Diamond Film Microcells Micromachined with Femtosecond laser: Application to the Determination of Water Framework Directive Metals

Amel Sbartai[1,4], Philippe Namour[1,2], Abdelhamid Errachid[1], Jan Krejči[7], Romana Šejnohová[7], Louis Renaud[3], Mohamed Larbi Hamlaoui[4], Anne-Sophie Loir[5], Florence Garrelie[5], Christophe Donnet[5], Hervé Soder[6], Eric Audouard[6], Julien Granier[6], Nicole Jaffrezic-Renault[1*].*

[1] University of Lyon, Institute of Analytical Sciences, UMR CNRS 5280, Université Claude Bernard Lyon 1, 43 boulevard 11 novembre 1918, F-69622, Villeurbanne cedex, France

[2] Irstea, UR MALY, 3bis quai Chauveau, CP 220, F-69336, Lyon cedex 09, France

[3] University of Lyon, Lyon Institute of Nanotechnology, UMR CNRS 5270, Université Claude Bernard Lyon 1, 43 boulevard 11 Novembre 1918, F-69622, Villeurbanne cedex, France

[4] University of Annaba, Laboratoire EPEV, BP 12, El Hadjar, 23000 Annaba, Algeria

[5] University of Lyon, Laboratoire Hubert Curien, UMR CNRS 5516, Université Jean Monnet Saint-Etienne, Saint-Etienne

[6] Société IMPULSION SAS, 12, rue Barrouin, 42000 Saint-Etienne

[7] BVT Technologies a.s., Hudcova 78c, 612 00 Brno, Czech Republic

RECEIVED DATE (to be automatically inserted after your manuscript is accepted if required according to the journal that you are submitting your paper to)

*Corresponding authors

Telephone: +33 472448306, fax: +33 472441206,

e-mail addresses: philippe.namour@univ-lyon1.fr; nicole.jaffrezic@univ-lyon1.fr.

ABSTRACT

Planar electrochemical microcells were micromachined in a microcrystalline boron-doped diamond (BDD) thin layer using a femtosecond laser. The electrochemical performances of the new laser-machined BDD microcell were assessed by differential pulse anodic stripping voltammetry (DPASV) determinations, at the nanomolar level, of the four heavy metal ions of the European Water Framework Directive (WFD): Cd(II), Ni(II), Pb(II), Hg(II). The results are compared with those of previously published BDD electrodes. The calculated detection limits are 0.4, 6.8 5.5 and 2.3 nM, and the linearities go up to 35, 97, 48 and 5nM for, respectively, Cd(II), Ni(II), Pb(II) and Hg(II). The detection limits meet with the environmental quality standard of the WFD for three of the four metals. It was shown that the four heavy metals could be detected simultaneously in the concentration ratio usually measured in sewage or runoff waters.

KEYWORDS: DPASV, laser micromachining; BDD; Planar microcell; heavy metal ions; Water Framework Directive.

1 Introduction

With a concern for sustainable development and the eco-design of instruments installed in the natural environment, the analytical methods involving toxic compounds must be banned, such as “heavy metals”, in particular mercury impregnation or films, even if the quantities used are relatively low. Indeed, substances such as cadmium or mercury have been classified as “priority hazardous substances” in the Decision N° 2455/2001/EC [1] and Directive 2008/32/CE [2], for which Member States should implement necessary measures with the aim of ceasing or phasing out emissions, discharges, and losses into water of those priority hazardous substances which derive from human activities. So it is preferable to banish these hazardous substances from our devices, rather than quibble over low or negligible implemented quantities and to be vigilant about the potential toxicity of any new substances used in our devices.

Furthermore, development of new devices using priority hazardous substances leads to a commercial dead-end and a waste of time and money: they cannot be used in Europe and even in the other parts of the world. Indeed, mercury is recognized as a chemical of global concern. U.S. Environmental

Protection Agency's Roadmap for Mercury (July 5, 2006) promotes reducing mercury in processes and products, even where cost-effective substitutes do not exist. The overall goal of the Global Mercury Partnership of the United Nations Environment Programme (Governing Council Decision 25/5, Nairobi, Kenya, 16-20 February 2009) is to reduce and eventually eliminate mercury use in products and processes and raising awareness of mercury-free alternatives. Among these products, electric and electronic devices are targeted. Because of these environment and regulatory concerns, mercury-free electrodes have become more attractive.

So, electrodes made of boron doped diamond (BDD) are extensively investigated for environmental and electroanalytical applications, because of their analytical properties, as low background current and a wide potential window in aqueous solutions (~ -1.35 to +2.3 V versus the normal hydrogen electrode)[3] corrosion stability in aggressive media and resistance to biofouling [4]. Unfortunately, films of BDD have to be prepared at high temperatures of about 800°C or above, using microwave assisted plasma-enhanced chemical vapor deposition (MPECVD).

The microstructuring of deposited thin films in microcells is usually made by photolithographic techniques that allow using photosensitive resins and selective chemical attacks (lift-off technique). Photolithographic techniques are well established and used to achieve excellent resolution, a magnitude order of one micrometer, but request several steps in a clean room environment, with each of these steps introducing a risk of error. In addition, some materials, especially carbon materials, are not chemically etched. These steps are time consuming; furthermore, they require preparations of chemical reagents and their disposal, and each new design requires the manufacture of a new set of masks, which complicates the process.

In this article we describe a new manufacturing process for electrochemical microcells micromachined by a femtosecond laser, which starts from a thin film of carbon deposited on an insulating layer of silicon.

Microelectrodes forming the microcell have sizes of a few hundred of micrometer, which is quite feasible by laser machining. Achieving direct machining has a significant advantage over

conventional photolithography, because only one step is needed to make all electrochemical microcells, the process is fast and without chemical reagent. Another characteristic of direct machining is that the computer controls the path of the laser beam relative to the work-piece. This helps one to obtain quickly and accurately repeatable structures and whether changes are needed and can quickly be modified to change the program control of the laser accordingly.

These new electrochemical microcells micromachined by a femtosecond laser will be applied to detection of metals cited in the Water Framework Directive (WFD) that governs European water policy. WFD has been in place as the main European regulation for the protection of water resources and the water environment since 2000 [5]. One of its principal objectives is to achieve good chemical and ecological status and to restore water bodies to a "good status" by 2015. Chemical status refers to specific pollutants (e.g., priority substances or priority hazardous substances) for which environmental quality standards (EQS) are proposed and defined for pollutants as minimum requirements [6].

As the WFD implementation gradually comes into effect in European countries, the environmental metrology market is bound to increase over the coming years. Consequently, faced with the magnitude of this metrological challenge and the urgency of the situation, a paradigm shift is required in order to imagine a new approach to the problem of water monitoring. Given this situation, current research on microsensors is leading to the emergence of many measuring principles. The Swift report (http://www.swift-wfd.com), published in December 2006, lists a wide range of monitoring methods currently available or under development for supporting the WFD.

In this work the analytical characteristics of electrochemical microcells micromachined by a femtosecond laser will be determined for cadmium, mercury, nickel, and lead using differential pulse anodic stripping voltammetry (DPASV).

2 Materials and Methods

2.1 Reagents

Cadmium AAS standard solution in 2% nitric acid, at 1000 mg/L, mercury AA/ICP standard solution for environmental analysis, in 9.4% nitric acid, at 995 mg/L, nickel AA standard solution in 0.9%

nitric acid, at 1000 mg/L, and lead ICP/DCP standard solution in 0.9% nitric acid, at 9954 mg/L, used for BDD evaluation, sulphuric acid (H_2SO_4) 95-97%, and hydrogen peroxide (H_2O_2) 30% used for cleaning, and potassium citrate used in the buffer were provided from Sigma-Aldrich (l'Isle d'Abeau Chesnes, France). Nitric acid (HNO_3) 68% and hydrochloric acid (HCl) 37% were provided from VWR International (Fontenay-sous-Bois, France).

2.2 Microcell Preparation

The work focused on achieving integrated planar electrochemical microcells made of a film of 300 nm of boron-doped microcrystalline diamond to 1300 ppm (BDD) deposited on an insulated silicon wafer of 4" in diameter. BDD electrodes were purchased from Adamant Technologies (La Chaux-de-Fonds, Switzerland). Polycrystalline boron-doped diamond (boron concentration higher than 1000-1300 ppm) of 300 nm thickness was grown by MPECVD on silicon coated with a isolating layer of silicon oxide and silicon nitride ($Si/SiO_2/Si_3N_4$) of 0.5 µm thickness. The electrodes were cut up from the BDD wafer by micromachining [7]. This one was conducted by IMPULSION SAS Company using a femtosecond laser (5 kHz, 2.5 W, 800 nm, 150 fs); a scanner head; a set of XYZ moving plates. The parameters used during processing are power, 150 mW; optic scanner, 80 mm; and speed, 10-20 mm/s. The design of microcells distributed on the wafer and the structure of each BDD microcell, including the working electrode, counter electrode, and pseudo-reference electrode, are shown, respectively, in Figure S1 and Photo 1.

2.3 Electrochemical Measurements

2.3.1. Apparatus

A PalmSens sensor PC interface (Eindhoven, The Netherlands) was used to apply differential pulse voltammetry to the microcell. It was connected to a PC computer loaded with specific software. The electrochemical cell was a 5 µL cell made of PEEK, provided by BVT Technologies (Brno, Czech Republic). Instead of the conventional saturated calomel electrode (SCE), the device used a pseudo-reference made of BDD. An O-ring seal defined the measuring volume, and the electrical contacts were obtained by pressure on the front side of the BDD electrodes.

2.3.2. Measuring Conditions

Prior to the experiments and after each calibration concentration, the BDD microcells were cleaned in a piranha mixture (H_2SO_4 (95-97%)/ HNO_3 (68%) [V/V=3:1]) at 200–215°C for 1.5 h, subsequently heated to 80°C for 15 min in a mixture of H_2O_2 (30%)/ammonia (25%) [V/V=1:1] and finally ultrasound cleaned in distilled water, then in ethanol, and finally dried with nitrogen. Piranha mixture is very dangerous, being both strongly acidic and a strong oxidizer, it is extremely energetic and potentially explosive if not handled with extreme caution. It should not be discharged with organic solvent residues. Piranha mixture is prepared before use, applying the sulphuric acid first, followed by the peroxide. Mix the solution in a hood with the sash between you and the solution. Wear gloves and eye protection. Handle with care.

Daily, BDD microcells had to be cleaned and activated by 10 mL of Piranha solution, a mix of H_2SO_4 (95-97%)/H_2O_2 (30%) [V/V=7:3] for 5 min. BDD microcells were then rinsed with distilled water, dried with nitrogen, and activated by cyclic voltammetry in 0.1 M HNO_3. Finally, DPASV was used for all determinations. Instrumental parameters and standard measuring conditions were performed in 0.1 M potassium citrate/HCl buffer, at pH 2; deposition potential and time were -1.7 V and 20 s; start and end potentials were -1.7 & 0.5 V; pulse amplitude & time are 50 mV & 0.01 s, voltage step: 10 mV and sweep rate 0.05 V/s. The potential of accumulation was usually chosen at -1.7 V and applied for 20 s. Preliminary studies showed that a short deposition time minimized possible interactions between metals during the accumulation phase (data not shown). As previous works, Mannivannan *et al.* [8] showed that potentials and peak intensities are modified when metals are mixed, and the calibration curves were determined with the four metals together. Indeed in our case voltammograms obtained from the mixture of the four metals show potential peaks shifted, with respect to the pure metals of 2.1%, 1.4%, 1.9%, respectively, for cadmium, lead, and nickel, except for mercury whose potential is shifted nearly 50%.

The calibration curves were obtained by diluting the standard stock solution of the mixed four metals (Cd, Hg, Pb, and Ni) in buffer covering the linearity range suspected. According to the standard ISO 15839:2003 [9], the limit of detection (LD) was determined as the average blank value plus three time the standard deviation of the voltammetric signal (peak current) of the lowest level standard. Dividing the minimum detectable signal by the slope of the calibration curve provided the

minimum detectable concentration or limit of detection. The limit of linearity was determined by performing standard additions of adequate concentrations on a blank solution, until nonlinearity of the resulting graph was evident. The resulting calibration curves were validated for the linear model according to the French standard method AFNOR XPT 90-210 [10]. The fit of the Cochran test to the linear model was performed with a risk of α error equal to 1%.

3 Results and Discussion

3.1 Morphological Characterization of BDD Microcell

SEM image of BDD surface (Photo S1) shows the microcrystalline structure. The mean crystal size is in the range of 100 nm. Some large crystals appear. The SEM image of a micromachined groove is presented in Photo 2; its width is around 50 µm. the BDD layer, insulating layer, and silicon substrate clearly appear along the groove.

3.2 Electrochemical Characterization of BDD Microcells

The working potential window is an important electrode property for ASV because it dictates which metal ions can be detected. For carbon electrodes, the anodic limit in most aqueous media is determined by the potential at which oxygen evolution occurs and the cathodic limit is determined by the potential at which hydrogen evolution commences. The reduction of dissolved oxygen is also a parasitic cathodic reaction. The anodic potential limit is an important electrode property, particularly for the analysis of the more electropositive metal ions. The cyclic voltammograms for 0.1 M HNO_3 solution performed with our BDD microcell (Figure S2) clearly shows that this one presents a low background and a wide range of working potential, from –1.5 to +1.5 V (potential window of 3 V). Electron transfer with the ferro/ferricyanide redox probe was tested. A voltammogram is presented in Figure S3. The microcell shows an anodic–cathodic peak separation ΔEp of 648 mV and a reversal peak current ratio of 1. The electron transfer is quite limited, due to the rather low doping rate of the microcrystallized BDD used.

3.3 Metal Detection Using DPASV

3.3.1 Optimization of Detection Conditions: Effect of pH

The measurement conditions were optimized of the four metals by varying the pH of 0.1 M citrate buffer with 0.1 M HCl solution. The behavior of four metals versus pH is shown in Figure S4. In more acid solutions, the lead and cadmium stripping peaks became increasingly sharper and more intense. It appears that the best measurement condition is acidic pH (pH = 2) for cadmium, lead, and nickel. But regarding nickel, the pH does not seem to affect the response, and for mercury the response is slightly stronger at neutral pH. These results clearly indicate that the type of buffer used have an effect on the DPASV peak current. Therefore, a 0.1 M citrate buffer (pH 2.0) was determined to be the optimum buffer solution.

The calibration curves for the four metals, obtained with the BDD microcell, at pH 2 are shown in Figure 1. The linear model was validated for the four metals, and the detection limits obtained for these four metals are, respectively, Cd, 0.37 nM; Ni, 6.8 nM; Pb, 5.5 nM; and Hg, 2.3 nM. The sensitivity is an important parameter for low detection limits; typically, a higher sensitivity will result in a lower limit of detection. The sensitivities calculated from calibration curves are in decreasing order equal to: Pb = 77 mA/M, Ni = 28 mA/M, Cd = 15 mA/M, and Hg = 9.3 mA/M. Another important analytical parameter to be compared is the linear dynamic range, which is assessed from calibration curves. The calibration curves are linear for all the metal ions, in a linear dynamic range of two orders of magnitude for Cd (linear up to 35 nM) and Ni (linear up to 97 nM), and one order of magnitude for Pb (linear up to 48 nM). Only mercury shows a relatively short linear range (linear up to 5 nM), but the detection of this latter metal has to be optimized (see below). Variation coefficients for Cd (20 nM), Pb (11 nM), Ni (38 nM), and Hg (0.55 nM) are respectively 11.4%, 3.2%, 0.8%, and 8.3%.

Comparing our results with those previously published about BDD electrodes shows the very low detection limits obtained with BDD microcells, except for mercury detection (Table 1).

3.3.2 Metal Detection by DPASV

In order to achieve higher detection sensitivity, we have employed the DPASV technique. This one increases the sensitivity by reducing capacitive current. A standard solution of (Cd^{2+}, Ni^{2+}, Pb^{2+},

Hg^{2+}) was used to evaluate the ASV responses of BDD microcells. These four metals are the metals identified as priority substances in the European Water Framework Directive (WFD). As the concentration of one metal can exert influences on the detection of the other metals [11], the calibration solution has been constructed to provide a concentration ratio of dissolved metals usually measured in sewage or runoff waters. According to data from Table S1, measured dissolved concentrations of Cd, Pb, and Ni are on average 15-50 times higher than those of mercury. Also, taking into account these data and sensitivities of DPASV measurements for each metal, we used a standard mixed stock solution with metal concentrations according to the following ratios 36/68/19/1 for, respectively, Cd/Ni/Pb/Hg. A general electrochemical spectrum obtained at the concentrations of dissolved Cd (21 nM), Ni (55 nM), Pb (1.1 nM), and Hg (0.55 nM) in 0.1 M potassium citrate/HCl buffer, pH 2, is shown in Figure 2. Well-defined, and slightly asymmetric, stripping peaks are obtained for all the metals. The peak-shape differences likely occur because of the manner in which the metal phase is formed and subsequently oxidized at the working electrode. The stripping peak potentials versus our pseudo-reference electrode, measured for the standard presented in Figure 2, are equal, respectively, for cadmium, nickel, lead, and mercury, to (average ± s; n=3): –1178 ± 25 mV (V%= 2.1%), -974 ± 21 mV (V%= 2.3%), -254 ± 16 mV (V%= 6.3%), and 119 ± 20 mV (V%= 16.8%) respectively. Variability is around 6-8% except for mercury where the peaks are small and potential variability is 25%. On BDD electrodes, the metal deposition form particles with some metal atoms having only metal–metal interactions and others having metal–diamond interactions. The polycrystalline nature of BDD, in terms of site heterogeneity and non-uniform electrical conductivity, gives a complex surface on which metal oxidation occurs. We attribute the asymmetric peak shape to variable electron-transfer kinetics across the surface whereby deposits of varying size are oxidized at different rates at different locations on the BDD surface. Consistent with this supposition is the fact that the stripping peak widths for BDD became narrower with decreasing scan rate [3].

Cadmium Detection

Figure 1 shows the calibration plot for 0.07-35 nM Cd(II) using a 20 s deposition time. Although cadmium calibration curve fits well to the linear model, at the error risk equal to 1%, the results seem

non-linear. This cadmium behavior using the BDD electrode has been already reported in the literature [12-13]. This may be attributed to the way cadmium settles onto diamond surface, depending on its concentration. This behavior, linked to nucleation and growth mechanisms during accumulation step, is well-known for lead or mercury deposited onto the electrode surface, and it is likely that cadmium behaves according to the same mechanism. At high cadmium concentrations, all the active sites on the diamond surface are probably saturated by cadmium, and growth of these nuclei is the principal deposition mechanism. At lower concentrations, the number of active sites on diamond surface may be changing with cadmium concentration, resulting in this nonlinear calibration. An alternative explanation for this nonlinear behavior may be competition, between cadmium and the three other metal ions in the standard solution, for the active sites on the BDD microcell surface. Indeed the calibration solution contains the four metals in the following ratios 36/68/19/1 for, respectively, Cd/Ni/Pb/Hg. According to Mannivanna *et al.* [8], the sequence of events during deposition and stripping from a solution containing both Pb and Cd could be as follows: 1) Pb tends to preferentially deposit on BDD during the accumulation stage; 2) Cd then deposits across the surface, directly on both BDD and Pb nanoparticles, which are already present on BDD; 3) during the stripping potential sweep, the Cd that was deposited directly on the BDD surface is stripped at the potential expected for Cd; 4) finally, at a more positive potential, the Cd that remains on the Pb nanoparticles is stripped along with Pb itself [8,11].

The BDD microcell presented gives the lowest detection limit for cadmium (LD: 0.4 nM) if we compared with data from Table 1. Indeed, El Tall *et al.* [11] found for cadmium a detection limit equal to 3 nM, for a deposition time of 60 s at -1.7 V, in acetate buffer 10 mM and a linear signal up to 200 nM. Other authors found higher detection limits on BDD electrodes (Table 1).

Lead Detection

Figure 1 shows the calibration plot for 5-50 nM Pb(II) using a 20 s deposition time. The BDD microcell gives a detection limit for lead (LD, 5.5 nM) among the lowest if compared with data from Table 1. Indeed, El Tall *et al.* [11] found for cadmium and lead, LD equal to 3 nM and 8 nM, respectively, for a deposition time of 60 s at -1.7 V, in acetate buffer 10 mM and a signal linear up to 200 nM. The deposition and anodic stripping detection by square-wave voltammetry of Pb on the

BDD electrode, in a 0.1 M HNO_3 solution, seem to be strongly enhanced by microwave activation. According to Tsai *et al.* [14], after a deposition time of 20 s, the LDs for Pb are equal to 0.1 nM and 1 nM, with microwave activation and without microwave activation, respectively. Recently, Chooto *et al.* [15] measured a LD of 1.5 nM for Pb on BDD by SWASV but after a deposition time of 7 min at -1.3 V. Yoon et al [16] propose a simultaneous detection of Cd, Pb, Cu and Hg in a solution of 0.1 M KNO_3 (pH 6) by DPASV on BDD electrode with a LD for Pb equal to 10 nM (E_{dep} = -1.5 V; t_{dep} = 5 min, scan rate 50 mV/s).

Nickel Detection

For nickel determination, our BDD microcell displays a detection limit of 6.8 nM. Zhang & Yoshihara measure Ni(II) ion concentrations in an electroless deposition bath using DPASV on a BDD rotating disk electrode. Their detection limit was 33 nM, for a deposition time of 60 s. The determination was carried out in alkaline solution (0.1 M NaOH + 0.1 M NH_4NO_3), and a regeneration electrode, after the detection, was carried out in 0.1 M H_2SO_4 [17].

Mercury Detection

Concerning mercury, the microcells are not very sensitive (LD: 2.3 nM for 20 s of deposition time) compared to Manivannan's team results where the LD is equal to 0.68 nM on the BDD electrode, but with 20 min of deposition time [18-19], and the detection limit reaches 0.05 nM using a rotating disk electrode and a deposition time = 60 s [20]. The same team, always on the BDD electrode calculate a LD equal to 0.02 nM with a deposition time of 5 min [21]. One origin to this low sensitivity of the BDD microcell under our operating conditions could be due to the presence of chloride ion in our buffer solution. Indeed the chloride ion and chloride and mercuric ions are known to form an insoluble calomel salt (Hg_2Cl_2) at the surface of the electrodes. This formation of calomel is a problem in all the electrodes used so far, including BDD. Obviously we can change the buffer composition, but chloride is an ubiquitous impurity and gold is an excellent metal which forms amalgam with mercury. To overcome this problem one solution is to co-deposit gold on the BDD electrode surface [19,21]. Other publications give detection limits close to ours: 3.5 nM for a deposition time of 5 min [16] and 3.2 nM of mercurous ion by cyclic voltammetry on BDD electrodes modified

with iridium oxide film [22]. Some improvements are necessary to optimize the response of these BDD microcells to mercuric ions.

The detection limits of BDD microcells are good both for regulatory and toxicity purposes. WFD proposes as minimum requirements Environmental Quality Standards (EQS) for Cd, Ni, Pb, and Hg and they are respectively 0.7-2.2 nM, 341 nM, 35 nM, and 0.25 nM; and the Predicted Non Effect Concentrations (PNEC) for water organisms are estimated to be: 1.9 nM, 8.5 nM, 1 nM, and 0.04 nM, respectively, for Cd, Ni, Pb, and Hg. Concerning regulatory purposes, the BDD microcell reaches the EQSs for cadmium, nickel, and lead. The detection limit of mercury needs to be lowered. With regard to aquatic organisms, toxicity thresholds (PNECs) are reached for cadmium and nickel but not for lead or mercury.

4 Conclusion

Planar electrochemical microcells were micromachined in a microcrystalline BDD thin layer using a femtosecond laser. They were designed for fitting in a flow-through cell. Sensing characteristics obtained with these laser micromachined BDD microcells are the same order of magnitude as those published in the bibliography, which are obtained with conventional electrochemical assemblies.

We showed how these microcells allow the detection of heavy metals in water, thus meeting the demand of the European Water framework directive. The simplicity of the DPASV technique on BDD microcells makes onsite monitoring of the heavy metal ions now a near-term reality.

Obviously, some improvements of this microcell are still possible and even needed: in particular, the potential for accumulation can be certainly optimized, the sensitivity to Hg ions must be increased, and finally microcells should be tested in a microfluidic system that should allow one to reduce the accumulation time and increase the sensitivity of the device.

These microcells have applications in electrochemical analysis not only in environmental water samples (e.g., natural and drinking waters, wastewaters, industrial waters) but their applications can be widened to biological samples for species directly detectable as electro-active species, heavy metals, and neurotransmitters. Other compounds could be detected, after electrode functionalization by synthetic or biological receptors.

5 Acknowledgements

The authors thank the French National Research Agency (ANR PRECODD Integreau n°0794C0100-101), 7th FP of European Union (INFULOC project n°230749) for their financial support and the Nanolyon technology platform.

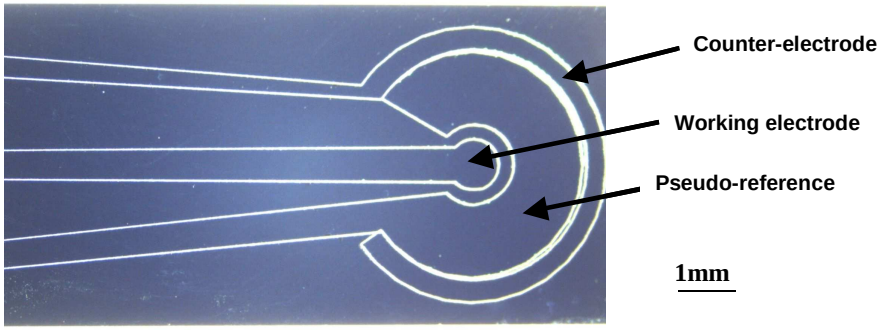

Photo 1: the three electrodes cut up from the BDD wafer by laser-machining, the working electrode is in centre, then around it the "reference", and finally the counter electrode on the edge.

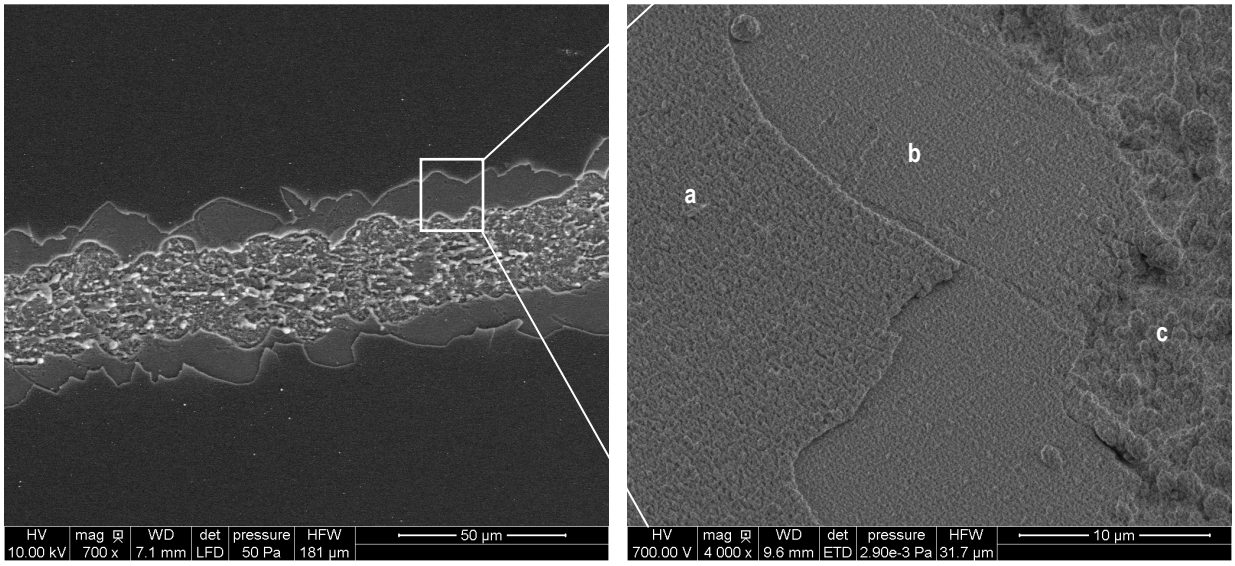

Photo 2: (Left) Femto laser micromachined groove; (Right) (a) BDD, (b) silicon nitride layers, and (c) silicon substrate, on the groove edge.

Table 1: Comparison of our results on BDD microcell with the published performances in scientific literature on BDD electrodes

Metal	Technique	Electrode	Doping (ppm)	Buffer	LD (nM)	Reference
Cd	DPASV	BDD	1 000 (10^{+20} cm^{-3})	0.1 M Acetate, pH 5.2	8.9	[3]
Cd	DPASV	BDD	810 [23]	0.1 M Acetate, pH 5.4	44	[24]
Cd	DPASV	BDD	10 000 [25]	0.2 M Acetate	355	[8]
Cd	DPASV	BDD	1300	0.01 M Acetate	3	[11]
Cd	DPASV	BDD	1300	0.1 M Acetate	8	[11]
Cd	DPASV	BDD	10 000 [25]	0.1 M KCl.	89	[12]
Cd	LSASV	Bi-BDD	1 000 (0.1%) Windsor Scientific	0.1 M $HClO_4$, pH 1.2	17	[26]
Cd	LSASV	BDD	0.1% in the source	0.1 M $HClO_4$	89	[27]
Cd	DPASV	BDD	No specified	0.1 M Acetate, pH 6	31	[16]
Cd	DPASV	BDD	1 300	0.1 M Citrate/HCl, pH 2	0.4	Our result
Hg	DPASV	BDD	No specified	0.1 M Acetate, pH 6.0	3,5	[16]
Hg	DPASV	BDD	10 000 (ref [25])	0.1 M KNO_3, pH 1	0,7	[18-19]
Hg	DPASV	BDD	No specified	1 M KCl, pH 4	0,05	[20]
Hg	ASV	IrOx-BDD	1 000 (0.1%) Windsor Scientific	0.1 M PO_4, pH 4	3,2	[22]
Hg	DPASV	BDD	10 000 [25]	1 M KCl, pH 4 + 4mg/L Au	0,02	[21]
Hg	DPASV	BDD	1 300	0.1 M Citrate/HCl pH 2	2.3	Our result
Ni	DPASV	BDD	10 000	0.1 M NaOH + 0,1 M NH_4NO_3	33	[17]
Ni	DPASV	BDD	1 300	0.1 M Citrate/HCl pH2	6.8	Our result
Pb	DPASV	BDD	1 000 (10^{+20} cm^{-3})	0.1 M Acetate, pH 5.2	24	[3]
Pb	DPASV	BDD	810 [23]	0.1M Acetate, pH 5.4	24	[24]
Pb	DPASV	BDD	10 000 [25]	0.1 M KCl pH 1	4	[28]
Pb	DPASV	BDD	10 000 [25]	0.2 M Acetate pH 5	251	[8]
Pb	DPASV	BDD	1 300	0.01 M Acetate	8	[11]
Pb	DPASV	BDD	1 300	0.1 M Acetate	46	[11]
Pb	DPASV	BDD	10 000 [25]	0.1 M KCl.	48	[12]
Pb	LSASV	Bi-BDD	1000 (0.1%) Windsor Scientific	0.1 M $HClO_4$, pH 1.2	11	[26]
Pb	LSASV	BDD	10 000 [25]	0.2 M KCl pH 1	1998	[29]
Pb	SWASV	BDD	1 000 (10^{+19} - 10^{+20} cm^{-3})	0.1 M HNO_3	101	[14]
Pb	SWASV	BDD	1 000 (0.1%) Windsor Scientific	0.2 M KNO_3 + 0.05 M HNO_3	1	[15]
Pb	DPASV	BDD	No specified	0.1 M Acetate,	10	[16]

				pH 6		
Pb	DPASV	BDD	1 300	0.1 M Citrate/HCl pH 2	5.5	Our result

1

2

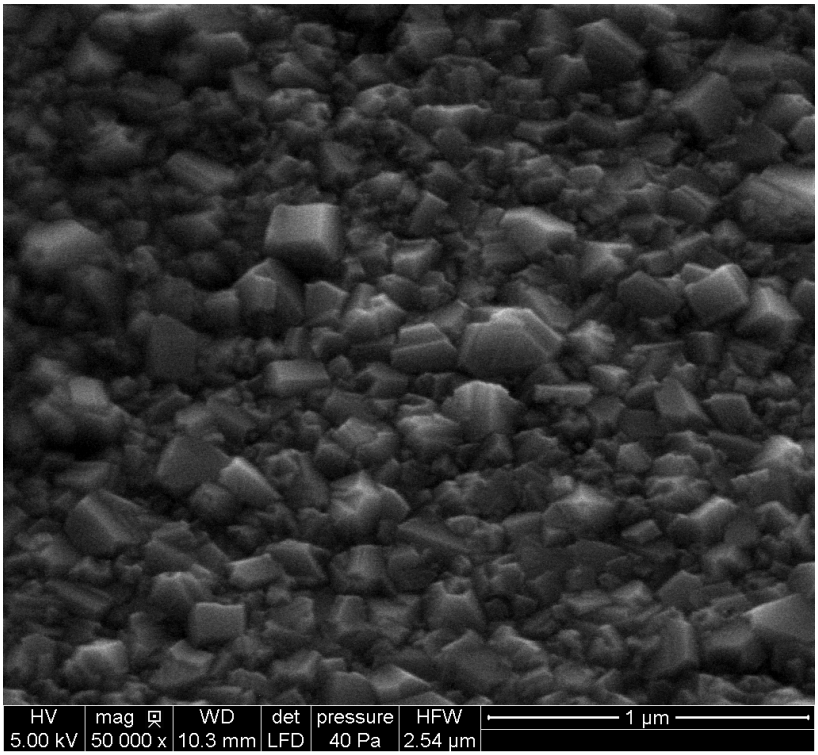

Photo S1: Morphological aspect of BDD layer

Table S1: Dissolved metal concentrations measured in wastewater (*), runoff water (**) and rainwater (***)

Cd (nM)	Pb (nM)	Ni (nM)	Hg (nM)	References
2**	37**	49**	-	[1]
-	-	-	2.4-1.3**	[2]
3.3***	7.6***	50***	-	[3]
4.4***	24***	44***	-	[4]
0.8**	11**	-	0.23**	[5]
-	7.1***	7.7***	-	[6]
4.7**	19**	-	-	[7]
0.6*	8.2*	110*	-	[8]
0.2***	1.1**	5**	-	[9]
-	-	-	0.023**	[10]
89**	91**	-	-	[11]

References cited

[1] Kayhanian, M.; Suverkropp, C.; Ruby, A.; Tsay, K., Journal of Environmental Management, 85 (2007) 279-295.
[2] Eckley, C. S.; Branfireun, B., Water Research, 43 (2009) 3635-3646.
[3] Báez, A.; Belmont, R.; García, R.; Padilla, H.; Torres, M. C., Atmospheric Research, 86 (2007) 61-75.
[4] Özsoy , T.; Örnektekin, S., Atmospheric Research, 94 (2009) 203-219.
[5] An, Q.; Wu, Y. Q.; Wang, J. H.; Li, Z. E., Environmental Monitoring and Assessment, 164 (2010) 173-187.
[6] Uygur, N.; Karaca, F.; Alagha, O., Atmospheric Research, 95 (2010) 55-64.
[7] Pagotto, C.; Legret, M.; Le Cloirec, P., Water Research, 34 (2000) 4446-4454.
[8] Houhou, J.; Lartiges, B. S.; Montarges-Pelletier, E.; Sieliechi, J.; Ghanbaja, J.; Kohler, A., Science of the Total Environment, 407 (2009) 6052-6062.
[9] Nimmo, M.; Fones, G. R., Atmospheric Environment, 31 (1997) 693-702.
[10] Zhang, J. F.; Feng, X. B.; Yan, H. Y.; Guo, Y. N.; Yao, H.; Meng, B.; Liu, K., Science of the Total Environment, 408 (2009) 122-129.
[11] Gnecco, I.; Berretta, C.; Lanza, L. G.; La Barbera, P., Atmospheric Research, 77 (2005) 60-73.

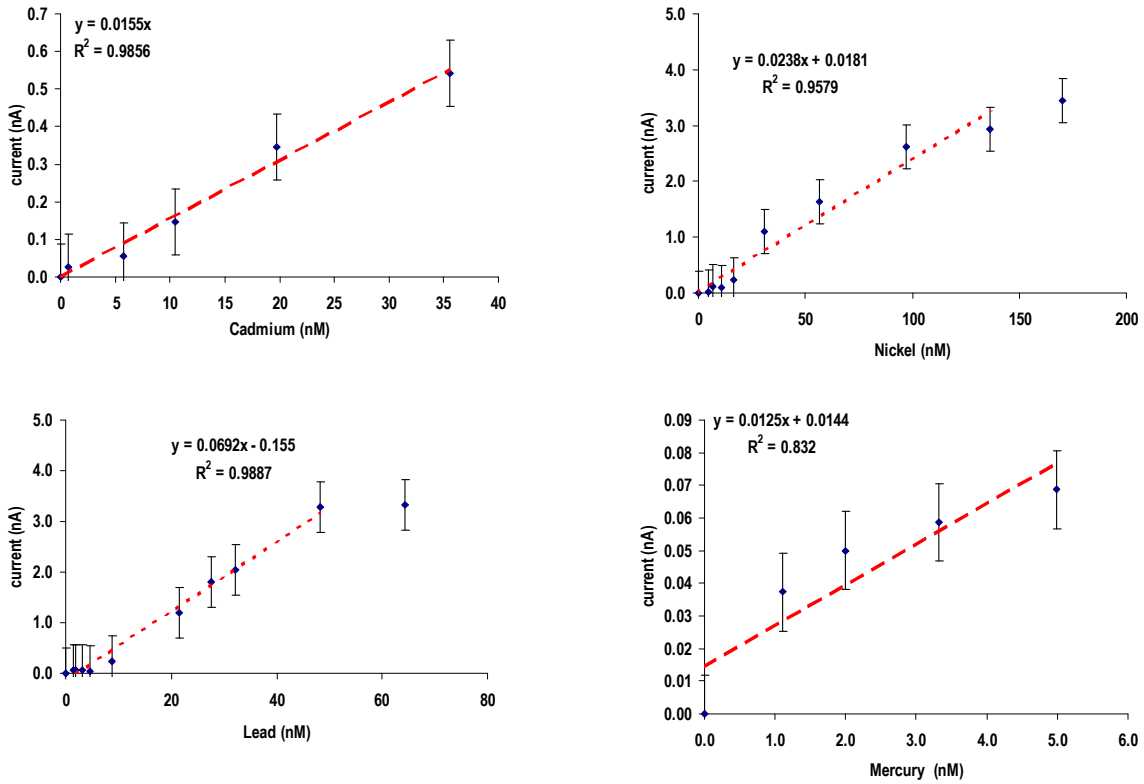

Figure 1: Calibration plots for Cd^{2+}, Ni^{2+}, Pb^{2+}, and Hg^{2+} ions at pH 2 in 0.1 M potassium citrate buffer: concentration range on the micromachined BDD microcell. Operating conditions: E_{dep} = -1.7 V; t_{dep} = 20 s; stripping at 50 mV/s.

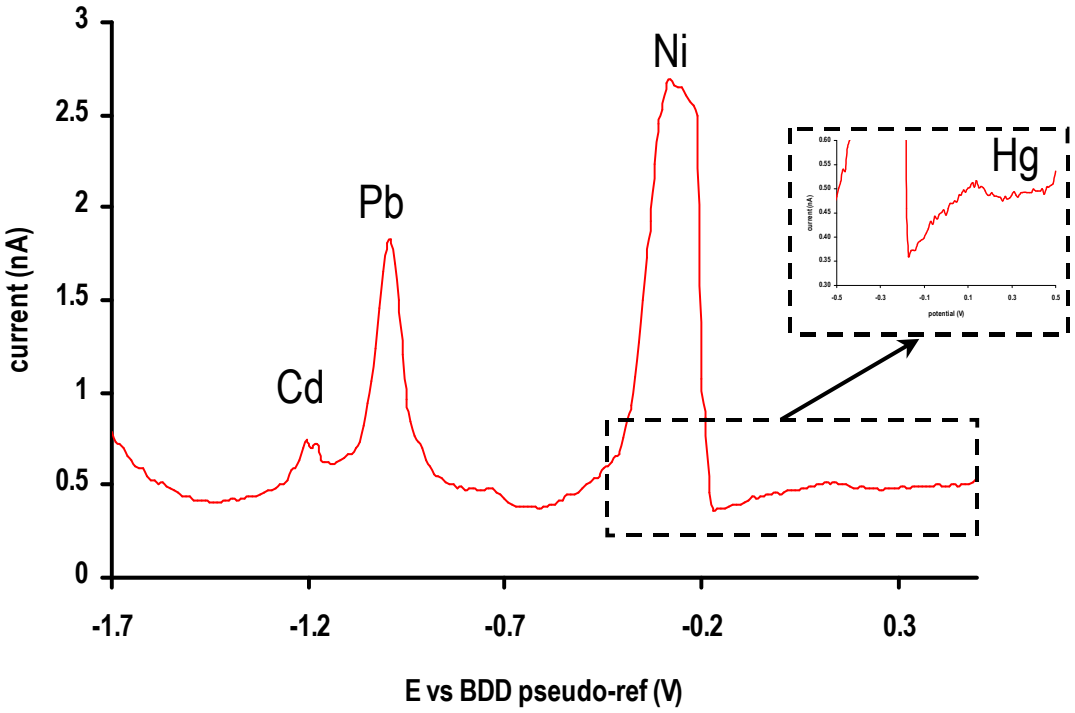

Figure 2: DPASV obtained with the BDD micromachined microcell, on a standard solution of Cd (20 nM), Ni (38 nM), Pb (11 nM), and Hg (0.55 nM) in 0.1 M potassium citrate/HCl buffer, pH 2; deposition potential and time: -1.7 V and 20 s; start and end potentials: -1.7 and 0.5 V; pulse amplitude and time: 50 mV and 0.01 s; voltage step: 10 mV; and sweep rate 0.05 V/s. The potential is measured versus a pseudo-reference electrode made of BDD.

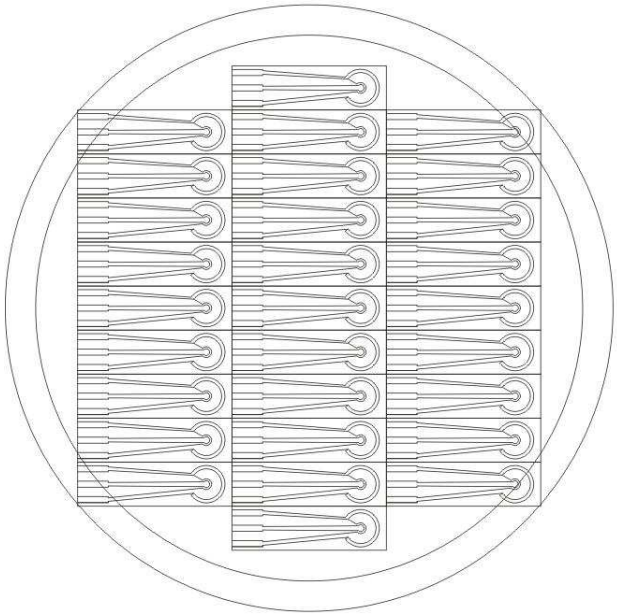

Figure S1: Design of electrochemical microcells distributed on a wafer of silicon insulated (4'' diameter)

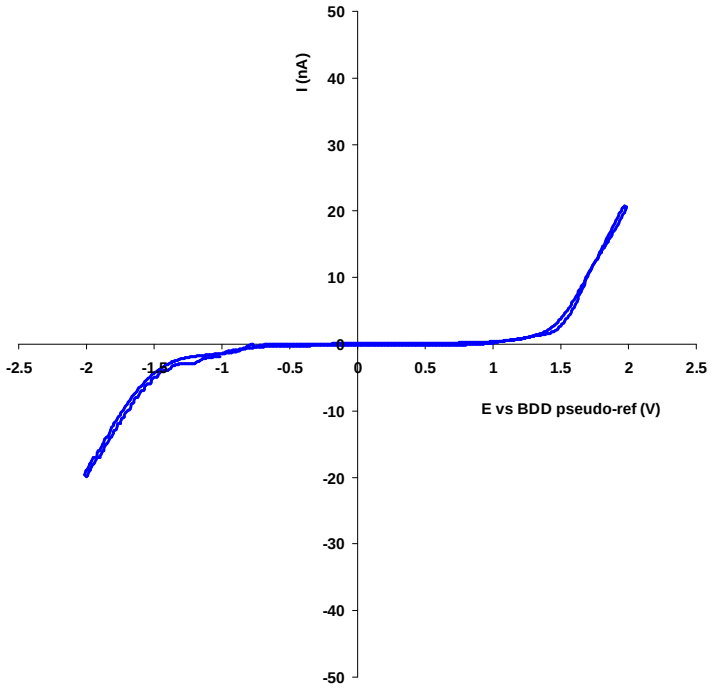

Figure S2: cyclic voltammograms for 0.1 M HNO_3 performed with a BDD microcell

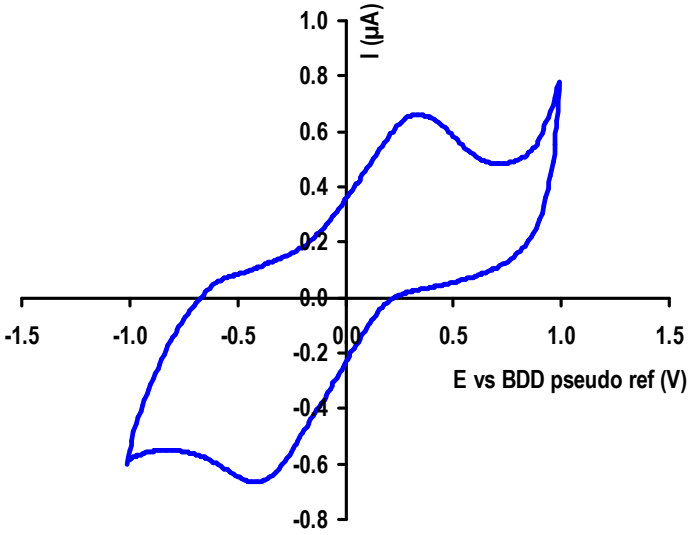

Figure S3: Cyclic voltammogram of 10 mM of ferro/ferricyanure in buffer solution (PBS 10 mM ; pH 7,4) with a scanning speed of 0.1 V/s.

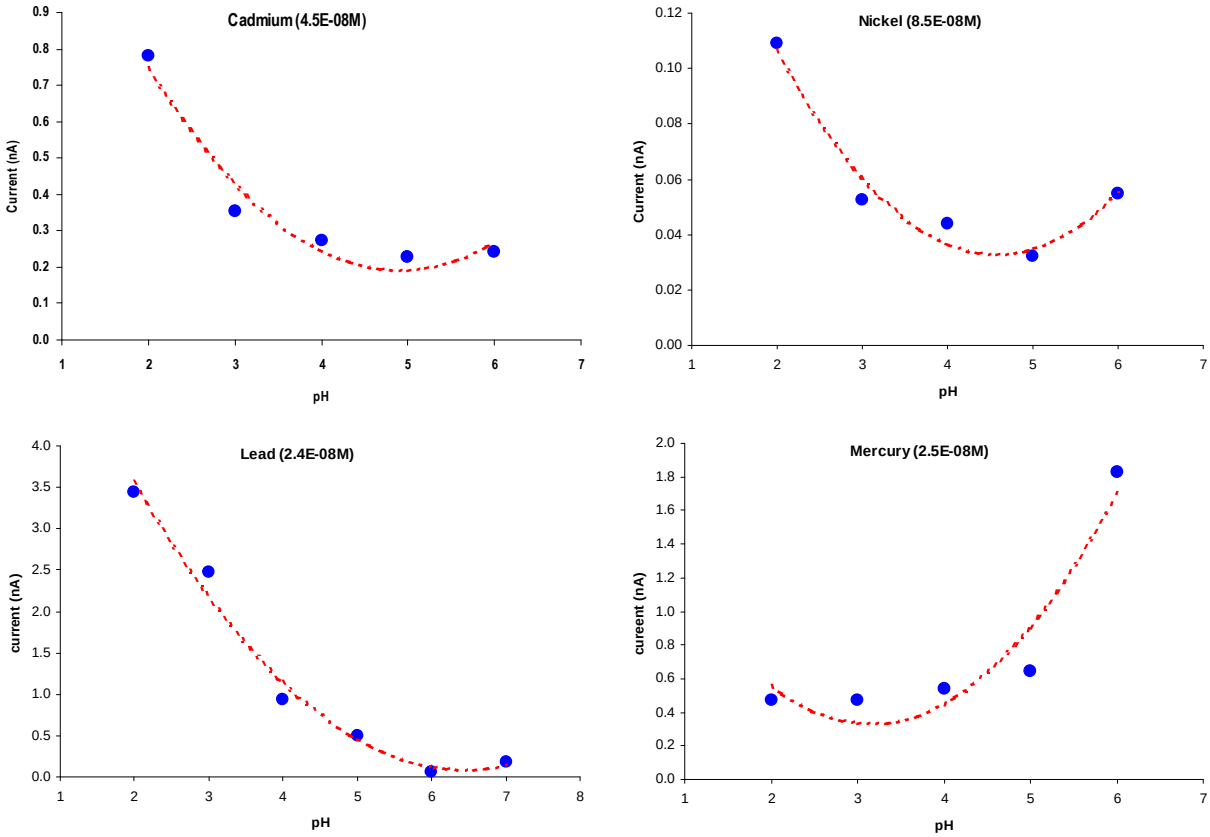

Figure S4: pH effect on the metal stripping peak (height in nA) for cadmium (45 nM), nickel (85 nM), lead (24 nM), and mercury (25 nM)

(1) OJEC; OJEC L 331, 2001; Vol. L331; pp 1-5.
(2) JOCE; JOCE L81 ed.; JOL, 2008; Vol. 2008/32/CE; pp 60-61.
(3) McGaw, E. A.; Swain, G. M. *Anal. Chim. Acta* **2006**, *575*, 180-189.
(4) Trouillon, R.; O'Hare, D. *Electrochim. Acta* **2010**, *55*, 6586-6595.
(5) JOCE In *Journal officiel des Communautés européennes*; JOL, 2000; Vol. 2000/60/CE; pp 1-73.
(6) JOCE In *Journal officiel des Communautés européennes*; JOC, 2008; Vol. Position Commune (CE) No 3/2008; pp 1-15.
(7) Jaffrezic-Renault, N.; Sbartai, A.; Errachid, A.; Renaud, L.; Namour, P.; Loir, A.-S.; Garrelie, F.; Donnet, C.; Soder, H.; Audouard, E.; Granier, J.: French Patent No. 1250807,France, 2012; pp 12.
(8) Manivannan, A.; Kawasaki, R.; Tryk, D. A.; Fujishima, A. *Electrochim. Acta* **2004**, *49*, 3313-3318.
(9) ISO In *n°15839*; ANFOR, 2006; Vol. NF EN ISO 15839; pp 38.
(10) AFNOR In *T 90-210*; AFNOR ed.; AFNOR, 2009; Vol. NF T 90-210; pp 43.
(11) El Tall, O.; Jaffrezic-Renault, N.; Sigaud, M.; Vittori, O. *Electronalysis* **2007**, *19*, 1152-1159.
(12) Babyak, C.; Smart, R. R. *Electronalysis* **2004**, *16*, 175-182.
(13) Toghill, K. E.; Xiao, L.; Wildgoose, G. G.; Compton, R. G. *Electronalysis* **2009**, *21*, 1113-1118.
(14) Tsai, Y. C.; Coles, B. A.; Holt, K.; Foord, J. S.; Marken, F.; Compton, R. G. *Electronalysis* **2001**, *13*, 831-835.
(15) Chooto, P.; Wararatananurak, P.; Innuphat, C. *ScienceAsia* **2010**, *36*, 150-156.
(16) Yoon, J. H.; Yang, J.; Kim, J.; Bae, J.; Shim, Y. B.; Won, M. S. *Bull. Korean Chem. Soc.* **2010**, *31*, 140-145.
(17) Zhang, Y. R.; Yoshihara, S. *Journal of Electroanalytical Chemistry* **2004**, *573*, 327-331.
(18) Manivannan, A.; Seehra, M. S.; Tryk, D. A.; Fujishima, A. *Anal. Lett.* **2002**, *35*, 355-368.
(19) Manivannan, A.; Seehra, M. S.; Fujishima, A. *Fuel Processing Technology* **2004**, *85*, 513-519.
(20) Manivannan, A.; Ramakrishnan, L.; Seehra, M. S.; Granite, E.; Butler, J. E.; Tryk, D. A.; Fujishima, A. *Journal of Electroanalytical Chemistry* **2005**, *577*, 287-293.
(21) Seehra, M. S.; Ranganathan, S.; Manivannan, A. *Anal. Lett.* **2008**, *41*, 2162-2170.
(22) Salimi, A.; Alizadeh, V.; Hallaj, R. *Talanta* **2006**, *68*, 1610-1616.
(23) Show, Y.; Witek, M. A.; Sonthalia, P.; Swain, G. M. *Chemistry of Materials* **2003**, *15*, 879-888.
(24) Sonthalia, P.; McGaw, E.; Show, Y.; Swain, G. M. *Anal. Chim. Acta* **2004**, *522*, 35-44.
(25) Yano, T.; Tryk, D. A.; Hashimoto, K.; Fujishima, A. *Journal of the Electrochemical Society* **1998**, *145*, 1870-1876.
(26) Toghill, K. E.; Wildgoose, G. G.; Moshar, A.; Mulcahy, C.; Compton, R. G. *Electronalysis* **2008**, *20*, 1731-1737.
(27) Fierro, S.; Watanabe, T.; Akai, K.; Yamanuki, M.; Einaga, Y. *Journal of the Electrochemical Society* **2011**, *158*, F173-F178.
(28) Manivannan, A.; Tryk, D. A.; Fujishima, A. *Electrochem. Solid State Lett.* **1999**, *2*, 455-456.
(29) Dragoe, D.; Spataru, N.; Kawasaki, R.; Manivannan, A.; Spataru, T.; Tryk, D. A.; Fujishima, A. *Electrochim. Acta* **2006**, *51*, 2437-2441.

1 Table of Contents Graphic
2
3

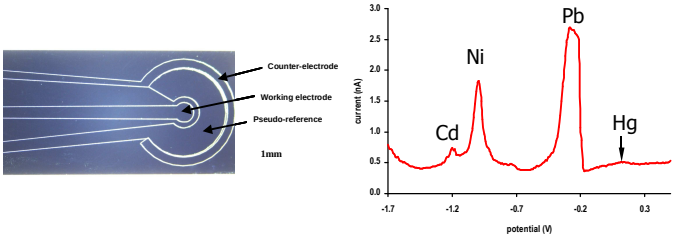

4